



## Strathprints Institutional Repository

**Hur, S. and Leithead, W.E. (2016) Collective control strategy for a cluster of stall-regulated offshore wind turbines. Renewable Energy, 85. 1260–1270. ISSN 0960-1481 , <http://dx.doi.org/10.1016/j.renene.2015.07.087>**

This version is available at <http://strathprints.strath.ac.uk/54003/>

**Strathprints** is designed to allow users to access the research output of the University of Strathclyde. Unless otherwise explicitly stated on the manuscript, Copyright © and Moral Rights for the papers on this site are retained by the individual authors and/or other copyright owners. Please check the manuscript for details of any other licences that may have been applied. You may not engage in further distribution of the material for any profitmaking activities or any commercial gain. You may freely distribute both the url (<http://strathprints.strath.ac.uk/>) and the content of this paper for research or private study, educational, or not-for-profit purposes without prior permission or charge.

Any correspondence concerning this service should be sent to Strathprints administrator: [strathprints@strath.ac.uk](mailto:strathprints@strath.ac.uk)

# Collective control strategy for a cluster of stall-regulated offshore wind turbines<sup>☆</sup>

S. Hur<sup>a,\*</sup>, W. E. Leithead<sup>a</sup>

<sup>a</sup>*Department of Electronic and Electrical Engineering, University of Strathclyde, Glasgow G1 1XW, United Kingdom*

---

## Abstract

1 The power converter is one of the most vulnerable components of a wind  
2 turbine. When the converter of an offshore wind turbine malfunctions, it  
3 could be difficult to resolve due to poor accessibility. A turbine generally  
4 has a dedicated controller that regulates its operation. In this paper, a  
5 collective control approach that allows a cluster of turbines to share a single  
6 converter, hence a single controller, that could be placed in a more accessible  
7 location. The resulting simplified turbines are constant-speed stall-regulated  
8 with standard asynchronous generators. Each cluster is connected by a mini-  
9 AC network, whose frequency can be varied through a centralised AC-DC-  
10 AC power converter. Potential benefits include improved reliability of each  
11 turbine due to simplification of the turbines and enhanced profit owing to  
12 improved accessibility. A cluster of 5 turbines is assessed compared to the  
13 situation with each turbine having its own converter. A collective control  
14 strategy that acts in response to the poorest control is proposed, as opposed  
15 to acting in response to the average control. The strategy is applied to a  
16 cluster model, and simulation results demonstrate that the control strategy  
17 could be more cost-effective than each turbine having its own converter,  
18 especially with optimal rotor design.

*Keywords:* offshore wind farm control, collective control, wind turbine control, wind turbine modelling, stall-regulated wind turbines.

---

<sup>☆</sup>This work was supported by the UK EPSRC (the Supergen Wind Energy Technologies Consortium) Platform Grant EP/H018662/1.

\*Corresponding author

*Email addresses:* hur.s.h@ieee.org (S. Hur), w.leithead@strath.ac.uk (W. E. Leithead)

## 1. Introduction

19 There is much interest in renewable energy due to concern over the envi-  
20 ronment, and wind is considered to be one of the most promising renewable  
21 energy sources. One of the reasons is that wind is an infinite and free source  
22 of energy with no harmful waste products. A wind turbine converts the ki-  
23 netic energy from the wind into mechanical energy. It is then converted into  
24 electricity, which is sent to a power grid. There are two basic configurations,  
25 vertical and horizontal-axis wind turbines. This paper is concerned with  
26 horizontal-axis wind turbines, having three blades [1]. The yaw mechanism,  
27 which is responsible for orientating the turbine towards the wind, is ignored  
28 in this paper.

29 The power converter is one of the most vulnerable components of a wind  
30 turbine. When the converter of an offshore wind turbine develops a fault, it  
31 could be difficult to repair due to accessibility problems, e.g. as a result of  
32 bad weather, etc. Normally, a wind turbine is equipped with a dedicated full  
33 envelope controller that regulates its operation. In this paper, a collective  
34 control approach that allows a cluster of (5 to 10) wind turbines to share  
35 a single converter (hence a single controller), which could be located in a  
36 place where it is more accessible away from the turbines, is proposed. Main-  
37 taining a dedicated power converter for an individual turbine and placing  
38 each of them away from the turbines (i.e. for improved accessibility) would  
39 be significantly more expensive, and, therefore, a single converter is shared  
40 between all the turbines in a cluster. The resulting simplified turbines are  
41 constant-speed stall-regulated [2] machines with standard asynchronous gen-  
42 erators. Constant-speed and stall-regulated turbines are known to be more  
43 reliable than variable-speed and pitch-regulated turbines, respectively. Each  
44 cluster is connected by a mini-AC grid (or network), whose frequency can be  
45 varied through a centralised AC-DC-AC power converter.

46 A number of clusters with its own dedicated mini-grid would be linked to  
47 constitute an offshore wind farm, which could subsequently be interconnected  
48 with an onshore wind farm through an appropriate transmission system.  
49 Various types of transmission system can be found in the literature, including  
50 the ones that exploit the high-voltage direct current (HVDC) [3, 4, 5], but  
51 this topic is not discussed in this paper.

52 The AC frequency of the cluster is altered by a controller responding to  
53 measurements of generator torque (or generator power) from each turbine  
54 within the cluster, thus, varying the rotor speed of the turbine. If each

55 turbine experienced the same wind speed, the regulation of each turbine  
56 would be almost identical to the situation with each turbine having its own  
57 converter and controller. However, each turbine experiences a different wind  
58 speed, and, therefore, the operational state of each turbine deviates from  
59 the required control strategy to the extent that drive-train torque and rotor  
60 speed transients are increased. When the cluster size becomes too large, the  
61 regulation would become unacceptable.

62 The idea of sharing a single converter between several turbines is not  
63 common but has been considered in the literature. In [6, 7] a single converter  
64 is also shared between several turbines but for different purposes; that is, for  
65 the purpose of re-powering smaller old wind turbines (e.g. 35 kW turbines)  
66 and for the purpose of reducing fluctuations on the wind farm power output  
67 in above rated wind speed (whereas the full operational envelop of wind speed  
68 is considered in this paper) focusing on the generator, respectively. In this  
69 paper, the impact of the proposed collective control strategy on the turbines'  
70 operation, including power efficiency and loads on the turbines, is studied.  
71 Another significant difference between these studies and the study presented  
72 here is that in [6, 7], it is assumed that each turbine is capable of providing  
73 an individual control by pitching while all the stall-regulated wind turbines  
74 considered in this study share a single collective control, i.e. the sole control  
75 action here is the collective control. Moreover, since the turbines considered  
76 in [6, 7] are relatively small, it is assumed that each turbine experiences the  
77 same wind speed therein. In this study, each turbine is significantly larger,  
78 being a 5 MW machine, and the turbines are therefore placed approximately  
79 1 km apart. Hence, each turbine experiences a unique wind speed (although  
80 correlated to be realistic), significantly impacting on the control performance.

81 The main contribution of this paper can now be summarised as propos-  
82 ing, implementing and testing the set-up whereby a single power converter  
83 and the controller are shared between multiple turbines. The novel objective  
84 is achieved by the use of a collective control strategy that is further improved  
85 to take account of the worst performing turbines when necessary. Potential  
86 benefits include improved reliability of each turbine due to simplification of  
87 the turbines and increased profit as a result of improved accessibility. Reli-  
88 ability improves further due to the use of constant-speed and stall-regulated  
89 wind turbines as opposed to variable-speed and pitch-regulated wind tur-  
90 bines. Note that even though the wind turbines are constant-speed machines  
91 [8], a variable-speed operating strategy is exploited in this study because the  
92 frequency of each cluster can be altered through a centralised AC-DC-AC

93 power converter. The disadvantage is that the control of each turbine is  
94 deteriorated with implications of potentially reduced energy capture and in-  
95 creased loads. These disadvantages undoubtedly become greater as the size  
96 (i.e. the number of turbines) of the cluster increases. In this paper, a cluster  
97 consisting of 5 turbines is investigated in comparison to the situation with  
98 each turbine having its own converter and controller. In order to develop  
99 the proposed collective control scheme, a wind turbine controller based on  
100 an existing strategy is first designed and implemented; that is, this controller  
101 serves as the basis for the collective control scheme. The importance of the  
102 choice of rotor design on the performance of the collective control strategy is  
103 also discussed.

104 A modified version of the wind turbine reported in [9] is modelled in  
105 Matlab/SIMULINK<sup>®</sup> in Section 2. The parameters of the SUPERGEN  
106 Wind Energy Technologies Consortium (Supergen) 5MW turbine are ex-  
107 ploited. This model is subsequently utilised as a control model [10] for  
108 designing a full envelope controller for the turbine as reported in Section  
109 3. Model Predictive Control (MPC) [11] is chosen as the controller design  
110 algorithm. The process input and output are grid frequency and generator  
111 torque, respectively, in contrast to the standard control strategy in which  
112 the process input and output are generator torque demand and generator  
113 speed, respectively. A stall-regulated variable-speed operating strategy [12]  
114 over the whole operational envelope is designed for a single turbine and its  
115 performance assessed in Section 3.

116 Subsequently, a cluster model of 5 wind turbines is developed by replicat-  
117 ing the single turbine model in combination with a DNV-GL-Bladed (Bladed)  
118 model of the same turbine (i.e. Supergen 5MW exemplar wind turbine) in  
119 Section 4. Suitable stochastic models for the wind speeds for each turbine,  
120 taking account of the correct correlation for layout of the cluster, are incorpo-  
121 rated into the cluster model. As with the single turbine case, the plant input  
122 and output for the cluster are the frequency of the local network connect-  
123 ing the cluster and measurements of generator torque (or power) from each  
124 turbine, respectively. A collective control strategy for the cluster of turbines  
125 that acts in response to the turbines with the poorest control when necessary  
126 is proposed, and the simulation results are compared with the situation with  
127 each turbine having its own converter and controller. Conclusions are drawn  
128 and future work discussed in Section 5.

## 129 2. Modelling

130 A simple Matlab/SIMULINK simulation model is developed in this sec-  
131 tion, based on the equations provided in [9]. This simplified model is the  
132 control design model exploited for designing the controllers in Sections 3 and  
133 4. Research is still being conducted to develop more detailed models to pre-  
134 dict wind turbines' response and performance more accurately [13, 14], but  
135 the controllers are still designed based on simplified models similar to the  
136 one reported in this section [15, 16, 17]. In fact, it is recommended that  
137 the control design model be kept not too complex since it could cause the  
138 controllers to be active at high frequencies and to lack robustness. A high  
139 fidelity aero-elastic model (of the same turbine) in Bladed is thus utilised to  
140 simulate the plant in Section 3. This model produces additional dynamics  
141 enabling further results to be obtained, including all significant variables and  
142 loads and lifetime equivalent fatigue load estimates.

143 The model employs the parameters of the 5MW exemplar wind turbine  
144 of Supergen. As the size of a cluster increases, each wind turbine would  
145 experience greater drive-train load transients and fluctuations in generated  
146 power in above rated wind speed as a result of increasing differences in the  
147 wind speed each turbine experiences. In order to ameliorate these effects  
148 to an extent, the model replaces the existing synchronous generator with an  
149 asynchronous induction generator since the latter would provide considerably  
150 greater damping.

### 151 2.1. Wind speed model

152 The wind stochastically varies with time and continuously interacts with  
153 the rotor [18]. The effective wind speed is wind speed averaged over the rotor  
154 area so that the power spectrum of aerodynamic torque remains intact. In  
155 this paper, it is derived by filtering the point wind speed [12] through the  
156 filter introduced in [18]. The point wind speeds that take account of the  
157 correlation of the cluster layout is obtained from Bladed. The effective wind  
158 speeds are required to simulate the Matlab/SIMULINK models in Section  
159 4. In Section 3, the wind is simulated in Bladed, and, thus, the effective  
160 wind speed model is not required. Turbulence intensity of 10% is employed  
161 throughout this paper.

162 *2.2. Aerodynamics*

The aerodynamic torque,  $T_f$ , has a nonlinear relationship with the effective wind speed,  $U$ , and the rotor speed,  $\Omega$ , as follows:

$$T_f = \frac{1}{2} \rho \pi U^2 R^3 \frac{C_p(\lambda)}{\lambda} \quad (1)$$

where the tip-speed ratio,  $\lambda$ , is defined as

$$\lambda = \frac{R\Omega}{U} \quad (2)$$

163  $R$  denotes the rotor radius,  $C_p$  the aerodynamic power coefficient, and  $\rho$  the  
 164 air density. From equations (1) and (2), it is clear that, for each wind speed,  
 165 the maximum power is produced at the value of the tip-speed ratio for which  
 166 the aerodynamic power coefficient is at a maximum. Hence, the value of  $T_f$   
 167 that corresponds to the maximum power values is proportional to  $\Omega^2$ .

168 *2.3. Drive-train Dynamics*

Rotor speed,  $\Omega$ , and generator speed,  $w_g$ , are dependent on aerodynamic torque,  $T_f$ , and generator reaction torque,  $T_e$  as follow

$$\begin{bmatrix} \Omega \\ w_g \end{bmatrix} = \begin{bmatrix} A(s) & B(s) \\ C(s) & D(s) \end{bmatrix} \begin{bmatrix} T_f \\ T_e \end{bmatrix} \quad (3)$$

The simplified model introduced here neglects the intermediate and high frequency components, and  $A(s)$ ,  $-B(s)/N$ ,  $C(s)/N$ , and  $-D(s)/N^2$  are reduced to

$$\frac{1}{((I_1 + N^2 I_2)s + (\gamma_1 + N^2 \gamma_2))} \quad (4)$$

169 where  $I_1$  ( $= 3.9 \times 10^7 \text{ kg m}^2$ ) denotes rotor inertia,  $I_2$  ( $= 534.1 \text{ kg m}^2$ ) gen-  
 170 erator inertia,  $N$  (97) gearbox ratio,  $\gamma_1$  ( $= 1.5 \times 10^5 \text{ Nm/rad/s}$ ) low-speed  
 171 shaft external damping coefficient, and  $\gamma_2$  ( $= 5 \text{ Nm/rad/s}$ ) high speed shaft  
 172 external damping coefficient.

173 *2.4. Induction Generator Unit Dynamics*

The model introduced in [9] includes a synchronous generator, but the model introduced here is modified to include an induction generator as previously mentioned. The the induction generator model is represented by the following equation

$$0.08\dot{T}_e + T_e = 5 \times 10^4 \left( w_g - \frac{f_g}{n_p} \right) \quad (5)$$

174 where  $f_g$  denotes the grid frequency and  $n_p$  the number of poles.

175 **3. Full Envelope Control**

176 The controller design for regulating variable-speed wind turbines could be  
177 categorised into two parts – the determination of the operating strategy of the  
178 controller and its synthesis. Recall that although the turbines are constant-  
179 speed machines, variable operating strategy is exploited in this study since  
180 the frequency of each cluster can be varied through a centralised AC-DC-  
181 AC power converter. The method of synthesis is Model Predictive Control  
182 (MPC) although other control algorithms, including Linear Quadratic Gaus-  
183 sian (LQG) [19], [20] and  $H_\infty$  [21], [22], would also be equally pertinent.

184 Normally, the determination of control strategy is more challenging as  
185 the implementation issues such as accommodation of the variation in turbine  
186 dynamics, and thus control regulation, over the full operational envelope,  
187 actuator constraints, which are most significant to the application, switching  
188 transients, start-up and shut-down all need to be identified and the controller  
189 realisation that best resolves them chosen. That is, this is related to nonlinear  
190 aspects of the turbine dynamics, and a careful investigation of the global  
191 behaviour of the system is essential. In this study, a control strategy that has  
192 been thoroughly tested and is currently in operation in real life is exploited.  
193 The details can be found in [23], but the control regulation and switching  
194 parts are briefly revised in this section.

195 *3.1. Rotor Characteristics and Control Strategy*

196 Two rotors having different aerodynamic characteristics are initially con-  
197 sidered. The aerodynamic power coefficients for Rotor A [9] and Rotor B  
198 (provided by Supergen) are presented in Figure 1, which demonstrates that  
199 Rotor A has a peaked  $C_p - \lambda$  curve whereas Rotor B has a broad flat  $C_p - \lambda$   
200 curve. The difference impacts greatly on the control strategy.



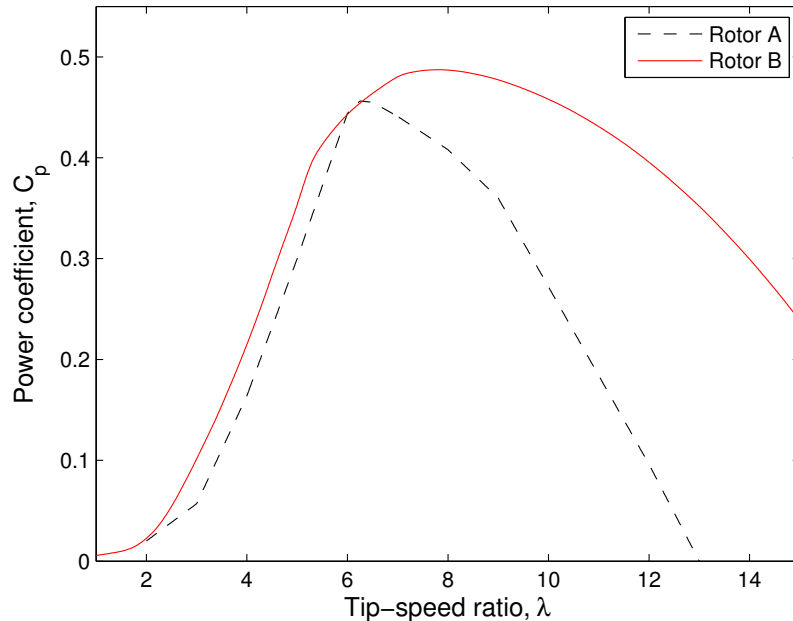


Figure 1:  $C_p - \lambda$  curves with flat and peaked characteristics.

201 The control strategies for both rotors are depicted in Figures 2 and 3.  
 202 For both, in mode 1, a constant rotor speed is maintained in the lowest wind  
 203 speeds; in mode 2, the rotor speed is varied to maximise the aerodynamic ef-  
 204 ficiency in intermediate wind speeds; in mode 3, constant rotor speed (higher  
 205 than the first mode) is again maintained in higher wind speed; in mode 4, the  
 206 rotor stalls to maintain rated power in above rated wind speeds. In Figure  
 207 2, mode 3 is only present to reduce the overshoot that could occur when  
 208 switching between modes 2 and 4.

209 Rotor A and Rotor B are, respectively, suitable for stall regulation and  
 210 pitch regulation because, as depicted in Figures 2 and 3, rotor speed needs  
 211 to be reduced much more rapidly as it switches from mode 3 to mode 4 with  
 212 Rotor B (i.e. the distance between mode 3 and the stall region is significantly  
 213 larger with Rotor B as depicted in the figures). However, when the number  
 214 of turbines in each cluster increases to 5, reduced energy capture cannot be  
 215 avoided. Rotor A is more vulnerable to reduced energy capture than Rotor  
 216 B since turbines with Rotor A need to operate much closer to the stall region

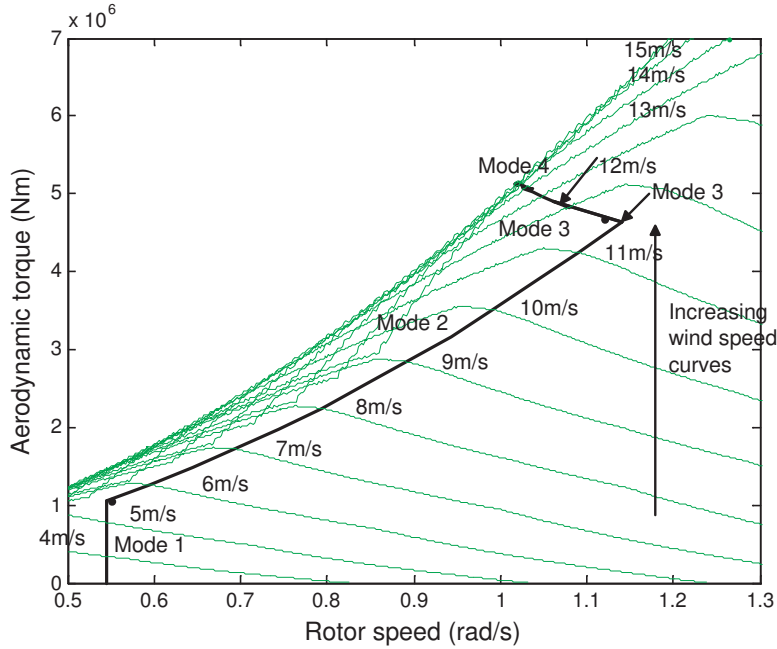


Figure 2: Operational strategy using Rotor A on the torque/speed plane.

217 as illustrated in the figures.

218 In summary, Rotor A provides improved results when there is only one  
 219 turbine in a cluster, and Rotor B outperforms Rotor A for a cluster of 5  
 220 turbines. Consequently, it would be appropriate to exploit a rotor that shares  
 221 the characteristics of Rotor A and Rotor B. Unfortunately, such a rotor is  
 222 not available for this study, and Rotor B is utilised throughout this paper to  
 223 maintain improved energy capture.

### 224 3.2. Control Regulation

In mode 2,  $T_f$  is caused to track the  $C_{pmax}$  curve. Because the  $C_{pmax}$  curve is proportional to  $\Omega^2$ , the corresponding output,  $y_i$ , which is also the input to the controller as depicted in Figure 4, is defined as follows [23]

$$y_i = T_{f,i} - k\Omega_i^2 \quad (6)$$

225 for  $i = 1, \dots, N$ , where  $N$  denotes the number of turbines in each cluster.

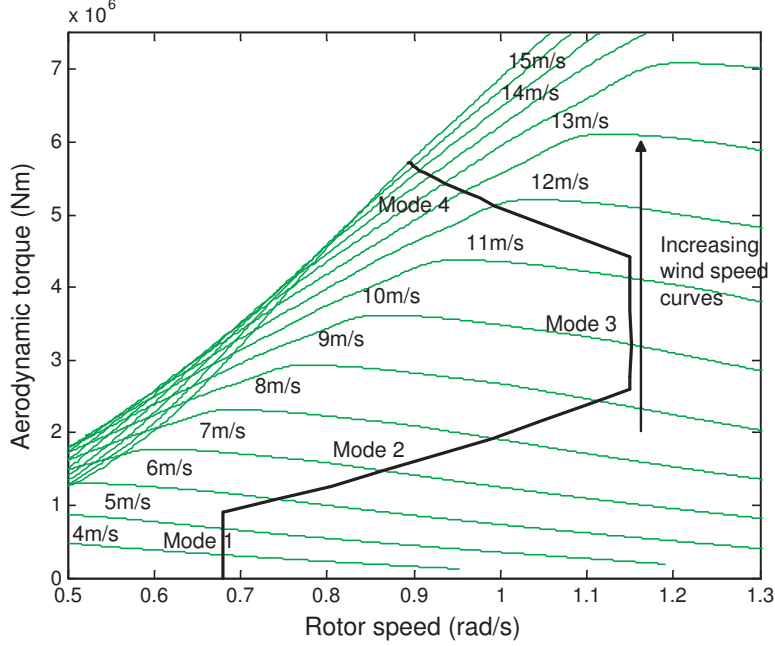


Figure 3: Operational strategy using Rotor B on the torque/speed plane.

$T_{f,i}$  cannot be directly measured and is, therefore, estimated from the measured drive-train torque,  $T_{e,i}$ . The equation thus becomes

$$y_i = NT_{e,i} + h(s)\Omega_i - k\Omega_i^2 \quad (7)$$

In order to obtain  $h(s)$ , equation (3) can be re-expressed as

$$T_{f,i} = \frac{\Omega_i}{A(s)} - \frac{B(s)}{A(s)}T_{e,i} \quad (8)$$

Since  $B(s) = -A(s)N$  (refer to equation (4)),  $T_{f,i}$  in equation (8) can be redefined as

$$T_{f,i} = A^{-1}(s)\Omega_i + NT_{e,i} \quad (9)$$

Hence,  $h(s)$  is obtained as

$$h(s) = \frac{1}{A(s)} \quad (10)$$

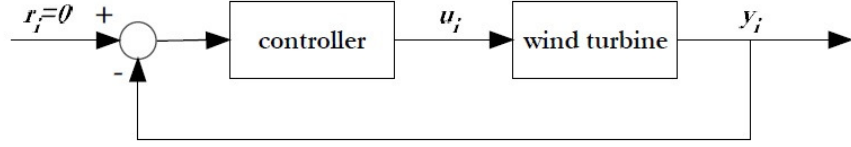


Figure 4: Control scheme.

However, since the derivative term in  $h(s)$  could amplify the high frequency noise, a low-pass filter is introduced, modifying  $h(s)$  in equation (10) as follows

$$h(s) = \frac{b}{A(s)(s + b)} \quad (11)$$

226 where  $b$  is in the range of 5 to 10 rad/s.

In mode 3,  $T_{f,i}$  is caused to track the constant rotor speed segment of the operating strategy curve shown in Figures 2 and 3. The corresponding output is, therefore, as follows

$$y_i = \Omega_i - \Omega_0 \quad (12)$$

227 where  $\Omega_0$  denotes the relevant constant rotor speed. This particular regu-  
 228 lation could lead to significant reduce energy capture, but it is necessary to  
 229 include this regulation since it enables smoother transition between modes 2  
 230 and 4.

In mode 4, the rated power,  $P_0$ , is maintained, in above rated wind speed, by causing  $T_{f,i}$  to track the constant power curve. The corresponding output is, therefore, as follows

$$y_i = T_{f,i} - \frac{P_0}{\Omega_i} \quad (13)$$

As with equation (7), equation (13) is modified to

$$y_i = T_{e,i} + h(s)\Omega_i - \frac{P_0}{\Omega_i} \quad (14)$$

231 *3.3. Linearisation*

From the nonlinear model introduced in Section 2, together with either equation (6), (12) or (14), depending on the mode of operation, a state space model can be linearised for the three operating points, modes 2, 3 and 4, as follows:

$$\begin{aligned}\Delta \mathbf{x}_{k+1} &= A\Delta \mathbf{x}_k + B\Delta u_k \\ \Delta y_k &= C\Delta \mathbf{x}_k\end{aligned}\tag{15}$$

where  $A$ ,  $B$ , and  $C$  are the state space matrices.  $\Delta y_k \in \mathbb{R}^n$ ,  $\Delta u_k \in \mathbb{R}^m$  and  $\Delta \mathbf{x}_k \in \mathbb{R}^r$  (where  $n$ ,  $m$ , and  $r$  are respectively 1, 3, and 1) are defined as

$$\Delta y_k = y_k - y_{k,o}\tag{16}$$

$$\Delta u_k = u_k - u_{k,o}\tag{17}$$

$$\Delta \mathbf{x}_k = \mathbf{x}_k - \mathbf{x}_{k,o}\tag{18}$$

232  $y_k$ ,  $u_k$ , and  $\mathbf{x}_k$  are the output, input, and states, respectively, and  $y_{k,o}$ ,  $u_{k,o}$ ,  
233 and  $\mathbf{x}_{k,o}$  are the operating points around which the models are linearised.  
234 The process input is the grid frequency, and the process output is  $y$ , which  
235 is generator torque, from either equation (6), (12) or (14) according to the  
236 wind speed.

For the sake of brevity, the equation can be rewritten as

$$\mathbf{x}_{k+1} = A\mathbf{x}_k + Bu_k\tag{19}$$

$$y_k = C\mathbf{x}_k\tag{20}$$

237 *3.4. Model Predictive Control*

For the linear model shown in equations (19) and (20), the prediction equations for MPC can be derived as [24]

$$\underbrace{\begin{bmatrix} \mathbf{x}_{k+1} \\ \mathbf{x}_{k+2} \\ \mathbf{x}_{k+3} \\ \vdots \\ \mathbf{x}_{k+n_y} \end{bmatrix}}_{\underline{\mathbf{x}}} = \underbrace{\begin{bmatrix} A \\ A^2 \\ A^3 \\ \vdots \\ A^{n_y} \end{bmatrix}}_{P_{xx}} \mathbf{x}_k + \underbrace{\begin{bmatrix} B_u & 0 & 0 & \cdots \\ AB_u & B_u & 0 & \cdots \\ A^2B_u & AB_u & B_u & \cdots \\ \vdots & \vdots & \vdots & \vdots \\ A^{n_y-1}B_u & A^{n_y-2}B_u & A^{n_y-3}B_u & \cdots \end{bmatrix}}_{H_{xx}} \underbrace{\begin{bmatrix} u_{k+1} \\ u_{k+2} \\ u_{k+3} \\ \vdots \\ u_{k+n_y} \end{bmatrix}}_{\underline{\mathbf{u}}}\tag{21}$$

and

$$\underbrace{\begin{bmatrix} y_{k+1} \\ y_{k+2} \\ y_{k+3} \\ \vdots \\ y_{k+n_y} \end{bmatrix}}_{\mathbf{y}} = \underbrace{\begin{bmatrix} C_g A \\ C_g A^2 \\ C_g A^3 \\ \vdots \\ C_g A^{n_y} \end{bmatrix}}_P \mathbf{x}_k + \underbrace{\begin{bmatrix} C_g B & 0 & 0 & \dots \\ C_g AB & C_g B & 0 & \dots \\ C_g A^2 B & C_g AB & C_g B & \dots \\ \vdots & \vdots & \vdots & \vdots \\ C_g A^{n_y-1} B & C_g A^{n_y-2} B & C_g A^{n_y-3} B & \dots \end{bmatrix}}_H \mathbf{u} \quad (22)$$

where  $n_y$  denotes prediction horizon, and  $\mathbf{u}$  is

$$[u_{k+1} \ u_{k+2} \ \dots \ u_{k+n_u-1} \ u_{k+n_u} \ u_{k+n_u} \ \dots \ u_{k+n_u}]^T \quad (23)$$

238 if control horizon,  $n_u$ , is smaller than prediction horizon,  $n_y$ . Prediction  
239 horizon  $n_y$  should not be smaller than  $n_u$ .

The control solution is obtained by minimising the following objective function [25]

$$J = \left\| r - H \mathbf{u} - P \hat{\mathbf{x}}_k - L \mathbf{d} \right\|_2^2 + \lambda \left\| \mathbf{u} \right\|_2^2 \quad (24)$$

subject to the following constraints

$$\underline{u}_i \leq u_i \leq \bar{u}_i \quad (25)$$

$$\Delta \underline{u}_i \leq \Delta u_i \leq \Delta \bar{u}_i \quad (26)$$

240 where  $\bar{u}_i$  and  $\underline{u}_i$  denote the upper and lower limits on  $u_i$ , respectively, and  
241  $\Delta \bar{u}_i$  and  $\Delta \underline{u}_i$  the upper and lower limits on  $\Delta u_i$ , the rate of change of input,  
242 respectively.  $r$  denotes the reference signal,  $H$  and  $P$  are from equation (22),  
243 and  $L$  is a vector of ones. The offset  $\mathbf{d}$  ( $= \mathbf{y} - \hat{\mathbf{y}}$ ) is included to produce  
244 unbiased predictions and offset correction. The first  $\|\cdot\|$  term is to reduce  
245 the reference tracking error and the second  $\|\cdot\|$  term to reduce the control  
246 action. Consequently,  $\lambda$  gives a trade-off between two conflicting problems.  
247  $\hat{\mathbf{x}}_k$  comes from the internal model here but the use of a state estimator such  
248 as the Kalman filter could also be appropriate.

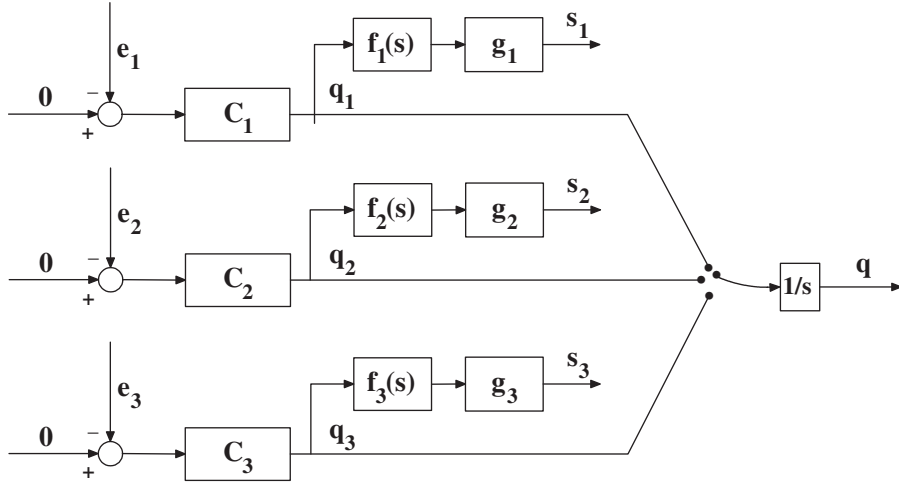


Figure 5: Switching procedure.

249 *3.5. Switching*

250 The controller needs to operate over the full operational envelope of wind  
 251 speed as described in Section 3.1. The MPC designed linear controllers are  
 252 combined through a switching procedure in a smooth manner that avoids the  
 253 introduction of large transients. One of the switching procedures introduced  
 254 in [23] is employed.

255 As illustrated in Figure 5, switching between the three Single Input Single  
 256 Output (SISO) controllers (i.e.  $C_1$ ,  $C_2$  and  $C_3$ , respectively for modes 2, 3  
 257 and 4) is required. The integral action, present in all the controllers, is  
 258 placed after the switch, thereby smoothing the discontinuities, which occur  
 259 on switching, and avoiding integral wind-up, which would otherwise occur  
 260 because the mean value of  $e_i$  (for  $i = 1, 2, 3$ ) is not zero when  $q$  acts in  
 261 response to  $q_i$  (for  $i = 1, 2, 3$ ). The difference in the spectra is partially  
 262 removed by the controllers  $C_1$ ,  $C_2$  and  $C_3$ , but a residual difference, mainly  
 263 due to the relationships of  $e_i$  (for  $i = 1, 2, 3$ ) to the wind speed, remains. The  
 264 filters,  $f_i(s)$  (for  $i = 1, 2, 3$ ), are designed to reduce this residual difference and  
 265 also the high frequency components of the spectra to reduce chattering due  
 266 to too rapid switching. Also, hysteresis needs to be incorporated to remove  
 267 chattering even further. Finally, the scaling constants,  $g_i$  (for  $i = 1, 2, 3$ ), are  
 268 present to adjust the relative distances to the curve.

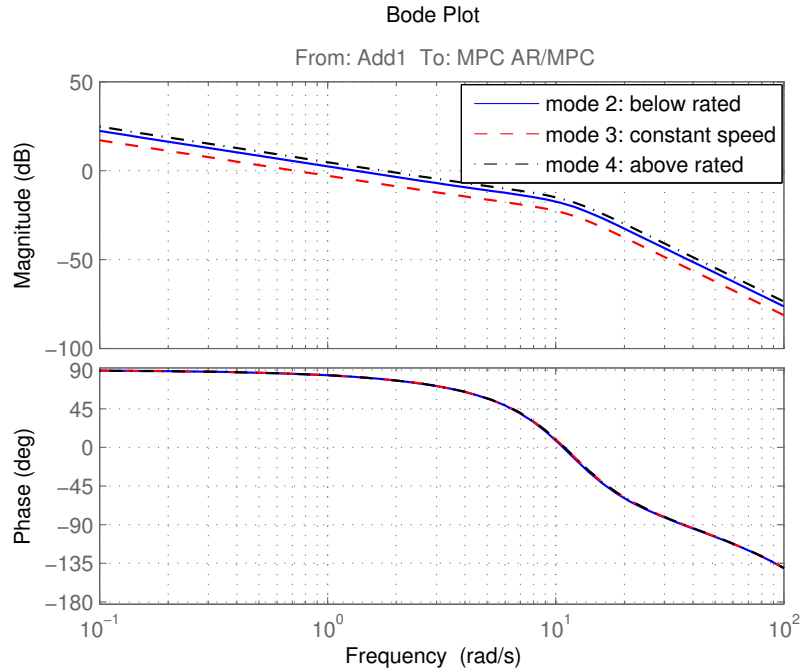


Figure 6: Open-loop frequency responses (the controller applied to the turbine model) in modes 2, 3 and 4.

### 269 3.6. Simulation Results

270 The controller is initially tuned through the application of the controllers  
 271 to the Matlab/SIMULINK model. The open-loop frequency response (the  
 272 controller applied to the model with open-loop) at each operating point is  
 273 depicted in Figure 6. Each gain crossover frequency is near 1 rad/s, which  
 274 implies that the control action would be neither too relaxed nor too aggressive  
 275 [26]. It is also indispensable to ensure that the controllers at each mode are  
 276 stable [27, 28]. As depicted in the figure, phase margins for the below rated  
 277 (mode 2), constant speed (mode 3) and above rated (mode 4) controllers are  
 278 approximately 81, 84 and 75°, respectively, indicating that their closed-loop  
 279 responses would be stable. Note that the MPC controllers incorporate a  
 280 positive feedback, i.e., the phase at the gain crossover frequency should be  
 281 added to a multiple of 360 degrees instead of 180 degrees to derive the phase  
 282 margin.

283 Once the controller is designed and tuned against the Matlab/SIMULINK



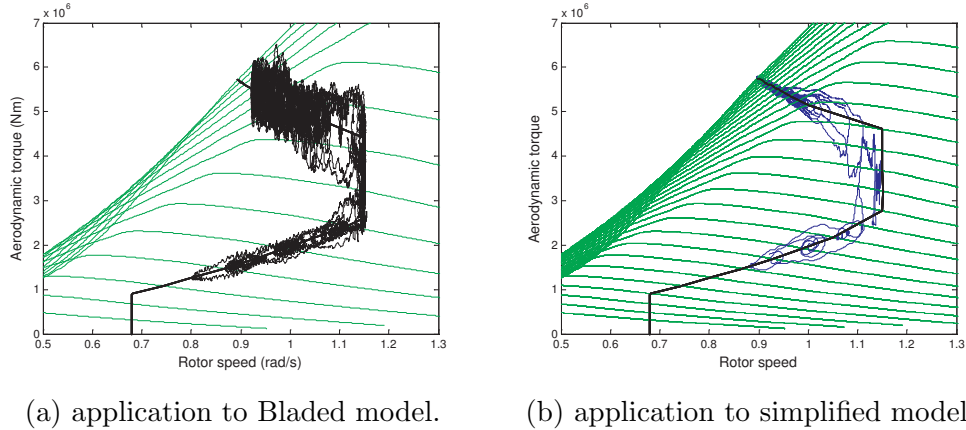


Figure 7: Behaviour of the turbine on the torque/speed plane.

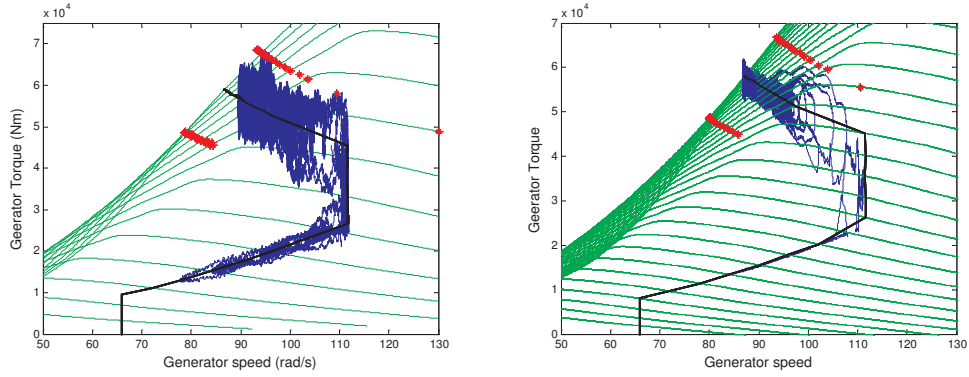
284 model (i.e. the control model), the controller is applied to the Bladed model  
 285 (i.e. the plant model of the same Supergen 5MW exemplar turbine) and  
 286 detuned. The differences between the control and plant models provide a  
 287 degree of model-plant mismatch to test the robustness of design. Moreover,  
 288 aero-elastic models, such as the plant model, includes more dynamics en-  
 289 abling further results to be obtained, including all significant variables and  
 290 loads and lifetime equivalent fatigue load estimates. Note that the use of  
 291 aero-elastic models is common in controller design before the application to  
 292 the real-life wind turbines. StrathControl Gateway, a commercial software  
 293 package that fully integrates the simulation, is utilised to allow the controller  
 294 designed in Matlab/SIMULINK to be applied to the Bladed model.

295 Figures 7 and 8 depict the behaviour of the control strategy on the  
 296 torque/speed planes [23]. In order to tune the controller, it is first applied  
 297 to the control design model, i.e. the simplified model developed in Mat-  
 298 lab/SIMULINK, as depicted in Figures 7b and 8b, and subsequently to the  
 299 Bladed model as shown in Figures 7a and 8a. Recall that the Bladed model  
 300 simulates the plant in this paper. The simulations in this section are carried  
 301 out at mean wind speeds of 8, 9, 11, 12, 14 and 16 m/s for the duration of  
 302 500 s.

303 As previously mentioned, the controller employs a switching mechanism  
 304 that has been tested exhaustively [23]. It is a switching mechanism that is  
 305 currently exploited in industry and is briefly revised in Section 3.5. Since

306 this rotor is not originally designed for stall-regulation, the overshoots that  
307 occur when switching, especially between mode 3 and mode 4, are inevitable.  
308 Nonetheless, the perturbations of aerodynamic power and generator power  
309 stay within acceptable 20% at wind speed above rated when applied to the  
310 Bladed model. Recall that the results can be improved significantly by util-  
311 ising Rotor A, but Rotor B needs to be used here because Rotor B outper-  
312 forms Rotor A when there are 5 turbines in a cluster, as discussed in the  
313 following section. The difference between the results when the controller is  
314 applied to the Matlab/SIMULINK and Bladed models mainly arises from  
315 rotational sampling and unsteady aerodynamics, which are included in the  
316 Bladed model only. Rotational sampling and unsteady aerodynamics should  
317 not impact on the control design [2], and thus it is evident that the use  
318 of a simplified model is sufficient for designing a wind turbine controller.  
319 Moreover, successful application to the Bladed model demonstrates that the  
320 controller designed based on the simplified model is robust. This controller  
321 serves as the basis for the collective control strategy introduced in Section 4.

322 The power efficiency at wind speed below rated cannot be obtained from  
323 Bladed simulations since the effective wind speed [18], required for the cal-  
324 culation of the power efficiency, is not available. However, it is illustrated in  
325 [29] that the power efficiency obtained by applying the controller to the Mat-  
326 lab/SIMULINK model, instead, provides almost identical results. Therefore,  
327 the power efficiency (through the application of the controller to the Mat-  
328 lab/SIMULINK model as opposed to the Bladed model) at wind speed below  
329 rated (i.e. 8 m/s) is plotted in Figure 9. It stays relatively high at above  
330 97.5%. Improvement is possible at the cost of “generator” power efficiency.  
331 The average power efficiency over time is 99.6% as shown in Figure 9.



(a) application to Bladed model. (b) application to simplified model.

Figure 8: Behaviour of the turbine on the torque/speed plane; red dots indicate  $\pm 20\%$  at wind speed above rated.

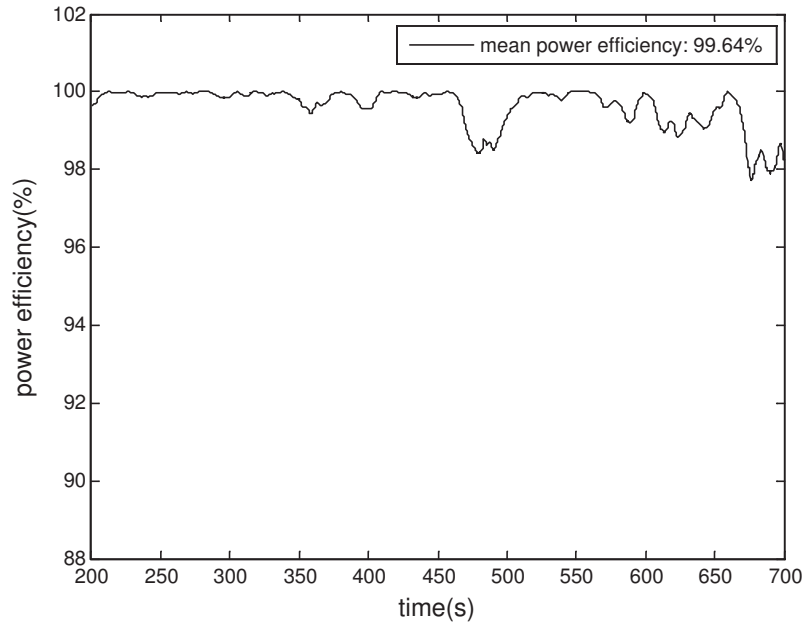


Figure 9: Power efficiency; 1 turbine in a cluster.

## 332 4. Collective Control

333 Initially, the controller designed in Section 3 has been applied to the model  
334 for a cluster of 5 wind turbines. It responds to the average of  $y_i (i = 1, \dots, N)$   
335 from equation (6), (12) or (14), depending on the current operating mode.  
336 In this approach, the controller tends to perform satisfactorily when  $N$  is  
337 relatively small. However, as it reaches 5, the performance becomes poorer  
338 because wind speed would be less uniform across a larger cluster than a  
339 smaller cluster, hence the difference between any  $y_i$  and the average would  
340 increase.

341 For improved results, a new collective strategy is introduced in this section  
342 to take into account the worst control by choosing  $y_i$  that is the furthest from  
343 the average when necessary. When wind speed is relatively uniform across the  
344 cluster, the average is chosen, otherwise, the controller chooses the turbine  
345 that is operating furthest from the average. The details of this strategy are  
346 described as follows, referring to Figure 10.

### 347 4.1. Collective Control Strategy

- 348 1. Error is defined as  $y_i (i = 1, \dots, N)$  from equations (6), (12) and (14),  
349 depending on the current operating mode. Average error is the mean  
350 of  $y_i (i = 1, \dots, N)$ . Largest error refers to the absolute largest error.
- 351 2. If the largest error is in Region BR1/AR1, the largest error is the  
352 control input. It improves the performance significantly over the use  
353 of the average error as the control input. In order to enable smoother  
354 transition between the largest errors, a low-pass filter is incorporated.  
355 Thresholds 1 and 4 are defined in the same way as defining the  $C_{pmax}$   
356 tracking curve in below rated wind speed; that is, using equation (6),  
357 but with a different  $k$ . Thresholds 2 and 3 are defined in the same way  
358 as defining the constant power curve in above rated wind speed, using  
359 equation (13), but with a different  $P_0$ .
- 360 3. If the largest error is in Region BR2/AR2, the average error is the  
361 control input. In this situation where wind speed is relatively uniform  
362 across the cluster, the use of the average error compared to the largest  
363 error improves the performance. If the largest error was used at all  
364 times, too much chattering would occur as the largest error “changes”  
365 – e.g. Turbine 1 has had the largest error so far, but now Turbine 2  
366 has the largest error. When the average error is tracked, the low-pass  
367 filter used in Region BR1/AR1 is no longer required.

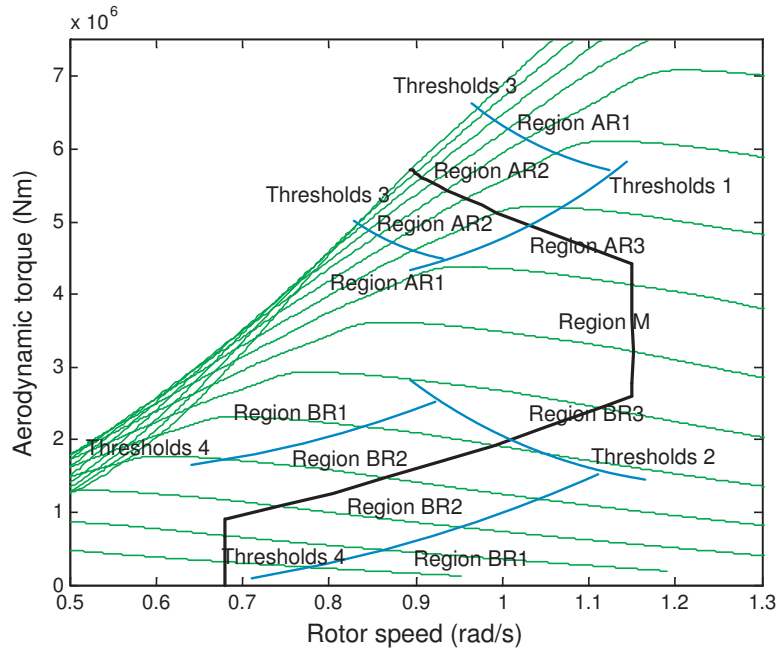


Figure 10: Collective control strategy.

- 368 4. If the average error is in Region BR3/AR3, the average error is used.  
 369 This is to enable a smooth transition between Region BR3/AR3 and  
 370 Region M; that is, if the largest error is used here, large transient  
 371 overshoots in torque occurs as switching takes place, in addition to  
 372 switching taking place incorrectly, i.e. at a wrong time.
- 373 5. To avoid chattering while crossing the thresholds, hysteresis needs to  
 374 be included between
- 375 • Region BR1 and BR2
  - 376 • Region AR1 and AR2
  - 377 • Region BR1&BR2 and Region BR3
  - 378 • Region AR1&AR2 and Region AR3
  - 379 • Region BR3 and Region M
  - 380 • Region AR3 and Region M

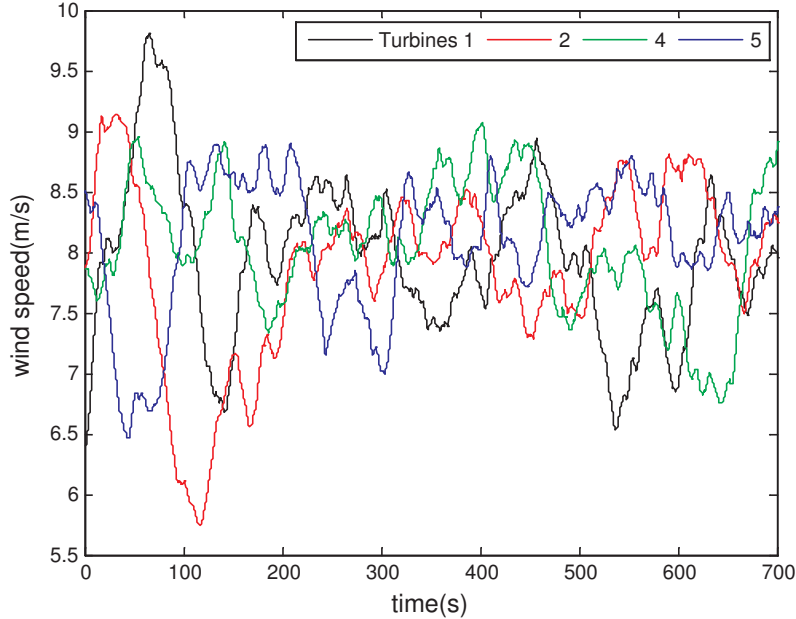


Figure 11: 4 effective wind speeds (mean of 8m/s) used with the Matlab/SIMULINK models, turbines 1, 2, 4 and 5.

381 *4.2. Simulation Results*

382 The Bladed model provides greater details for the structural loads, while  
 383 the Matlab/SIMULINK model enables many turbines to be included in a  
 384 cluster as previously mentioned. The cluster model thus consists of 4 Mat-  
 385 lab/SIMULINK models (introduced in Section 2) and 1 Bladed model (of the  
 386 same turbine). The two software packages are connected using StrathControl  
 387 Gateway, a commercial software package that fully integrates the simulation.  
 388 Modelling mismatch exists between the Bladed and Matlab/SIMULINK mod-  
 389 els, but it would also exist in real life. As introduced in Section 2, point wind  
 390 speeds are obtained using Bladed and filtered to produce effective wind speeds  
 391 to be incorporated into the Matlab/SIMULINK models. For the Bladed  
 392 model, this procedure is not needed since the software allows users to design  
 393 wind models more easily. 4 correlated wind speeds at a mean of 8 m/s, used  
 394 with the Matlab/SIMULINK models, are depicted in Figure 11. Similar wind  
 395 speeds are obtained for different mean wind speeds.

396 Simulations in this section are carried out at mean wind speeds of 8, 9.5,  
397 11, 12, 14 and 16 m/s. Although switching takes place at mean wind speeds  
398 of 10 and 12 m/s in the situation with each turbine having its own converter  
399 and controller, as shown in Section 3.6, in the situation where there are 5  
400 turbines sharing a set of converter and controller, switching takes place at  
401 different mean wind speeds of 9.5 and 11 m/s. Therefore, 9.5 and 11 m/s,  
402 instead of 8 and 10 m/s, are chosen. This is because at any mean wind speed,  
403 the range of rotor speed is significantly reduced as the collective controller  
404 responds to the average of  $y_i (i = 1, \dots, N)$  in comparison to the situation  
405 with each turbine having its own converter and controller.

406 Figures 12 and 13 depict the performance of the control strategy on the  
407 speed/torque planes. In comparison to the situation with each turbine having  
408 its own converter and controller, Figure 13 depicts greater drive-train load  
409 transients and larger fluctuations in generator power, especially in Turbines  
410 4 and 5, which cross over  $\pm 20\%$ . Referring to Figure 12, increased loads  
411 on the rotor can be surmised. Variance of the measurements of Turbine 3 is  
412 larger than the others since the Bladed model includes more dynamics than  
413 the Matlab/SIMULINK model, e.g. unsteady aerodynamics and rotational  
414 sampling.

415 The power efficiencies and their mean at wind speed below rated (i.e.  
416 8 m/s) are plotted in Figure 14 for each turbine. Turbine 3 is excluded  
417 here since the direct calculation of its power efficiency cannot be attained in  
418 Bladed, as explained in Section 3.6. Despite the increased number of turbines,  
419 they stay relatively high, with the average and the lowest power efficiencies  
420 exceeding 98 % and 95 %, respectively. When Rotor A is employed, the  
421 power efficiencies are significantly lower, with the average and the lowest  
422 power efficiencies not exceeding 80 % and 60 % [30]. This is the reason that  
423 Rotor B instead of Rotor A is utilised in this study even though Rotor A is  
424 more suitable for stall-regulated operations.

425 The results in this section depict that the performance of each turbine  
426 degrades compared with the situation with each turbine having its own con-  
427 verter and controller. However, the deficit as a result of this degradation  
428 could be outweighed by the savings that could be made by sharing a set of  
429 converter and controller among 5 turbines. Furthermore, the results would  
430 improve significantly if improved rotors can be utilised.

431 As each turbine experiences a different wind speed, the state of each tur-  
432 bine deviates from the required control strategy to the extent that drive-train  
433 torque and rotor speed transients are increased as previously mentioned.

Table 1: Performance indices for 1, 3 and 5 turbine wind farm

Number of turbines	Average duration outside the limits (%)	Largest deviation (%)
1	0	9.61
3	1.67	26.7
5	2.68	29.8

434 Clearly, the deviation should become larger as the number of turbines in-  
 435 creases, and turbines would eventually operate outside the 20% limits de-  
 436 picted (in red) in Figures 8 and 13. The average duration of the turbines'  
 437 operation outside the limits is tabulated in Table 1 for wind farms of 1, 3 and  
 438 5 turbines. Since the limits are only crossed when switching from modes 3  
 439 to 4, the average duration (in %) outside the limits is calculated only at the  
 440 mean wind speed at which the switching takes place. Moreover, the largest  
 441 deviation from the control design curve in percentage is also recorded in the  
 442 table. Note that the Matlab/Simulink model simulates the turbines for the  
 443 table. The result demonstrates that, as the number of turbines in each clus-  
 444 ter increases, the turbines deviate more both in time and magnitude from  
 445 the required control strategy as expected.



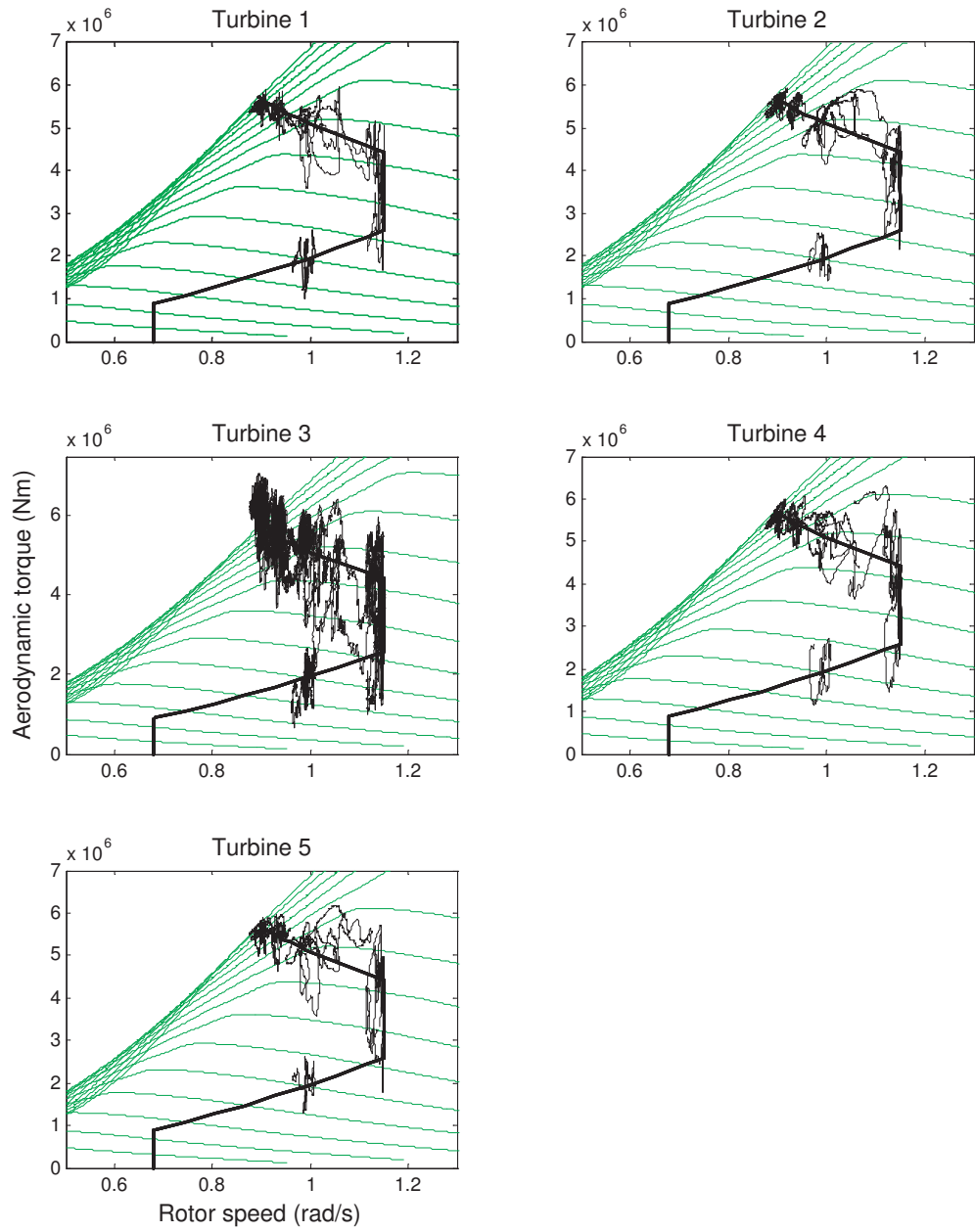


Figure 12: Turbines 1 to 5; Behaviour of each turbine on the torque/speed plane.

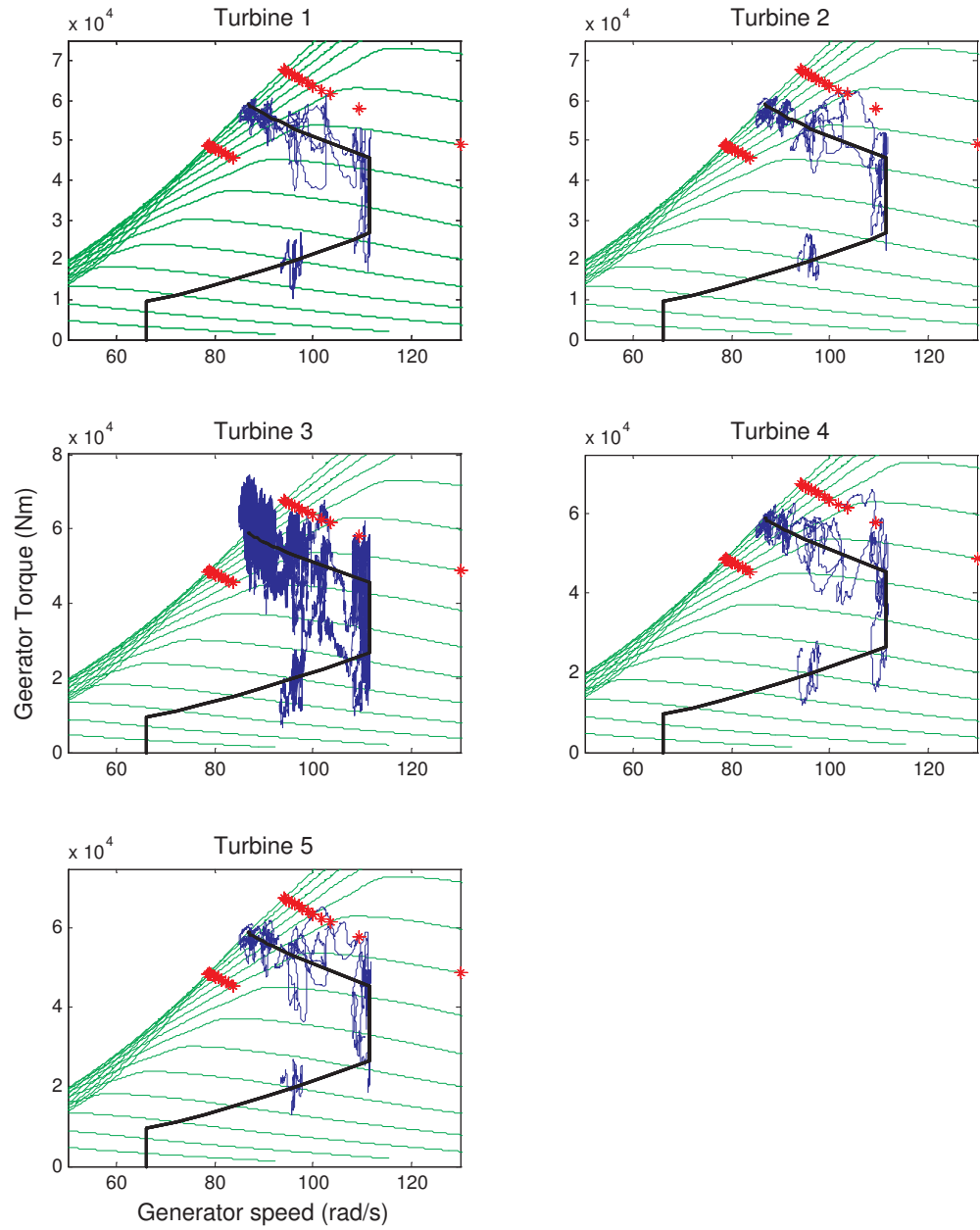


Figure 13: Turbines 1 to 5; Behaviour of each turbine on the torque/speed plane.

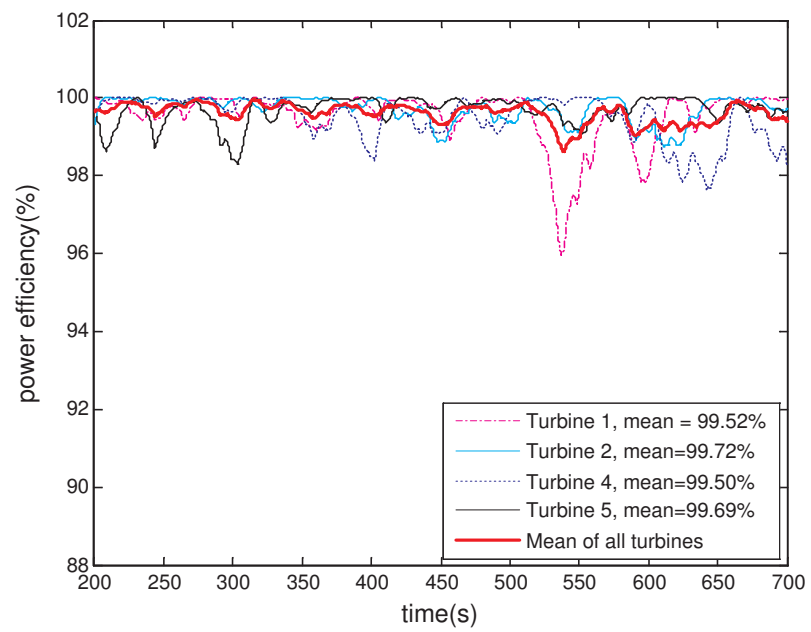


Figure 14: Power efficiency; 5 turbines in a cluster.

## 446 5. Conclusions and Future Work

447 Equations from [9] are exploited for modelling a nonlinear wind turbine.  
448 The parameters of the Supergen 5MW exemplar turbine are exploited. In  
449 order to provide greater damping – hence to ameliorate the effect of drive-  
450 train load transients and larger fluctuations in generated power as a result  
451 of having multiple turbines in a cluster – the model replaces the existing  
452 synchronous generator with an asynchronous induction generator.

453 An MPC based controller that operates over the full operational envelope  
454 of wind speed is designed based on the linearised models of this nonlinear  
455 model. It is first applied to a single turbine model (i.e. the Bladed model  
456 of the Supergen 5MW exemplar turbine), simulating a situation with each  
457 turbine having its own converter and controller. Subsequently, based on  
458 this full envelop controller, a collective controller for a cluster of 5 turbines,  
459 sharing a set of converter and controller, is designed. This collective control  
460 strategy acts in response to the poorest control when necessary as opposed  
461 to responding to the average control at all times. The strategy is assessed  
462 by application to a cluster model, consisting of 1 Bladed model and 4 Mat-  
463 lab/SIMULINK models. The Bladed model provides greater details for the  
464 structural loads, while the Matlab/SIMULINK model enables many turbines  
465 to be included in a cluster.

466 The simulation results demonstrate that the performance of each turbine  
467 degrades as expected in comparison to the situation with each turbine hav-  
468 ing its own converter and controller. However, the cost as a result of this  
469 degradation could be outweighed by the savings that could be earned by  
470 sharing a single set of converter and controller among 5 turbines. Moreover,  
471 the simulation results could improve significantly if optimal rotor design can  
472 be employed although such a rotor is not available for this study. Most im-  
473 portantly, the collective control strategy allows the power converter, which  
474 is one of the most vulnerable components of a wind turbine, to be sepa-  
475 rated from the turbines that are less accessible, e.g. due to bad weather, etc,  
476 and to be placed in a location where it is more accessible. Consequently,  
477 downtime as a result of potential generator problems would reduce, and the  
478 reliability of each turbine would improve due to simplification of the turbines.  
479 Reliability of each turbine is further improved by the use of constant-speed  
480 stall-regulated machines.

481 As future work, a rotor that is more suitable for the collective control  
482 strategy, i.e. a rotor that shares the characteristics of Rotor A and Ro-

483 tor B, could be developed. Furthermore, at the cost of increased compu-  
484 tational cost, more Bladed models could be employed to replace the Mat-  
485 lab/SIMULINK models since the Bladed model incorporates more dynamics  
486 enabling further results to be obtained, including all significant variables and  
487 loads and lifetime equivalent fatigue load estimates.

## 488 **Acknowledgements**

489 The authors wish to acknowledge the support of the EPSRC for the Super-  
490 gen Wind Energy Technologies Consortium, grant number EP/H018662/1.

## 491 **References**

- 492 [1] T. Burton, D. Sharpe, N. Jenkins, E. Bossanyi, Wind Energy Handbook,  
493 John Wiley & Sons, Ltd, 2001.
- 494 [2] F. D. Bianchi, H. D. Battista, R. J. Mantz, Wind Turbine Control  
495 Systems: Principles, Modelling and Gain Scheduling Design, Springer,  
496 2006.
- 497 [3] S. M. Muyeen, R. Takahashi, J. Tamura, Operation and Control of  
498 HVDC-Connected Offshore Wind Farm, IEEE Transactions on Sustain-  
499 able Energy 1 (1) (2010) 30 – 37.
- 500 [4] E. Veilleux, P. W. Lehn, Interconnection of Direct-Drive Wind Turbines  
501 Using a Series-Connected DC Grid, IEEE Transactions on Sustainable  
502 Energy 5 (1) (2014) 139 – 147.
- 503 [5] B. Silva, C. Moreira, L. Seca, Y. Phulpin, J. Peas Lopes, Provision of  
504 Inertial and Primary Frequency Control Services Using Offshore Mul-  
505 titerminal HVDC Networks, IEEE Transactions on Sustainable Energy  
506 3 (4) (2012) 800 – 808.
- 507 [6] A. Egea-Alvarez, O. Gomis-Bellmunt, Sensorless control of a power con-  
508 verter for a cluster of small wind turbines, in: Proceedings of the EWEA,  
509 Barcelona, 2014.
- 510 [7] T. Wakui, R. Yokoyama, Reduction in Power Output Fluctuations by  
511 a Parallel-Variable Speed Operation using Multiple Wind Turbines, in:  
512 Proceedings of the EWEA, Vienna, 2013.

- 513 [8] M. T. Iqbal, A. H. C. Coonick, L. L. Freris, Dynamic control of a stand-  
514 alone wind turbine, in: Proceedings of the 15th British Wind Energy  
515 Conference, York, UK, 1994, pp. 135 – 140.
- 516 [9] W. Leithead, B. Connor, Control of variable speed wind turbines: Dy-  
517 namic models, International Journal of Control 73 (13) (2000) 1173 –  
518 1188.
- 519 [10] C. Brosilow, B. Joseph, Techniques of Model-based Control, Prentice  
520 Hall Professional, 2002.
- 521 [11] M. Morari, C. Garcia, D. M. Prett, Model predictive control: Theory  
522 and practice-A survey, Automatica 25 (3) (1989) 335–348.
- 523 [12] I. Munteanu, A. I. Bratcu, N.-A. Cutululis, E. Ceangă, Optimal Control  
524 of Wind Energy Systems: Towards a Global Approach, Springer, 2007.
- 525 [13] X. Yang, F. Sotiropoulos, R. J. Conzemius, J. N. Wachtler, M. B. Strong,  
526 Large-eddy simulation of turbulent flow past wind turbines/farms: the  
527 Virtual Wind Simulator (VWiS), Wind Energy (2014) 1–21.
- 528 [14] F. Cuzzola, S. Aubrun, B. Leitl, Characterization of a wind turbine  
529 model for wake aerodynamics studies, Journal of Physics: Conference  
530 Series 555 (1) (2014) 1–7.
- 531 [15] Y. Nam, J. gi Kim, C. L. Bottasso, Maximal power extraction strategy in  
532 the transition region and its benefit on the AEP (annul energy product),  
533 Journal of Mechanical Science and Technology 25 (6) (2011) 1613–1619.
- 534 [16] B. M. Nagai, K. Ameku, J. N. Roy, Performance of a 3 kW wind turbine  
535 generator with variable pitch control system, Applied Energy 86 (2009)  
536 1774–1782.
- 537 [17] H. Camblong, Digital robust control of a variable speed pitch regulated  
538 wind turbine for above rated wind speeds, Control Engineering Practice  
539 16 (2008) 946–958.
- 540 [18] W. E. Leithead, Effective wind speed models for simple wind turbine  
541 simulations, in: Proceedings of 14<sup>th</sup> British Wind Energy Association  
542 (BWEA) Conference, Nottingham, 1992.

- 543 [19] P. Dorato, *Linear-quadratic Control: An Introduction*, Prentice Hall,  
544 1995.
- 545 [20] M. J. Grimble, M. A. Johnson, *Optimal control and stochastic estima-  
546 tion: theory and applications*, Wiley, 1988.
- 547 [21] J. W. Helton, O. Merino, *Classical Control Using  $H_\infty$  Methods: An  
548 Introduction to Design*, SIAM, 1998.
- 549 [22] S. Skogestad, I. Postlethwaite, *Multivariable Feedback Control: Analy-  
550 sis and Design*, 2nd Edition, Wiley, 2005.
- 551 [23] W. Leithead, B. Connor, Control of variable speed wind turbines: Design  
552 task, *International Journal of Control* 73 (13) (2000) 1189 – 1212.
- 553 [24] J. A. Rossiter, *Model-Based Predictive Control: a Practical Approach*,  
554 CRC Press, 2005.
- 555 [25] J. M. Maciejowski, *Predictive Control with Constraints*, Prentice Hall,  
556 2000.
- 557 [26] D. J. Leith, W. E. Leithead, Appropriate realization of gain-scheduled  
558 controllers with application to wind turbine regulation, *International  
559 Journal of Control* 73 (11) (1996) 1001–1025.
- 560 [27] T. Bakka, H. R. Karimi, S. Christiansen, Linear parameter-varying mod-  
561 elling and control of an offshore wind turbine with constrained informa-  
562 tion, *IET Control Theory Appl.* 8 (1) (2014) 22–29.
- 563 [28] M. Cai, Z. Xiang, H. R. Karimi, Robust Sampled-Data  $H_\infty$  Control for  
564 Vibration Mitigation of Offshore Platforms with Missing Measurements,  
565 *Mathematical Problems in Engineering* 2014 (2014) 1–10.
- 566 [29] A. P. Chatzopoulos, Full Envelope Wind Turbine Controller Design for  
567 Power Regulation and Tower Load Reduction, Ph.D. thesis, University  
568 of Strathclyde (2011).
- 569 [30] S. Hur, W. Leithead, Feasibility study of offshore wind farms using  
570 simplified turbine, The supergen wind energy technologies consortium  
571 report, Industrial Control Centre and UK Wind Energy Research - Doc-  
572 toral Training Centre, University of Strathclyde (2012).